Climatic Change (2007) 83:401–427
DOI 10.1007/s10584-006-9235-y

Regional modelling of future African climate north of 15°S including greenhouse warming and land degradation

Heiko Paeth · Hans-Peter Thamm

Received: 17 November 2004 / Accepted: 15 November 2006 / Published online: 8 February 2007

Abstract Previous studies have highlighted the crucial role of land degradation in tropical African climate. This effect urgently has to be taken into account when predicting future African climate under enhanced greenhouse conditions. Here, we present time slice experiments of African climate until 2025, using a high-resolution regional climate model. A supposable scenario of future land use changes, involving vegetation loss and soil degradation, is prescribed simultaneously with increasing greenhouse-gas concentrations in order to detect, where the different forcings counterbalance or reinforce each other. This proceeding allows us to define the regions of highest vulnerability with respect to future freshwater availability and food security in tropical and subtropical Africa and may provide a decision basis for political measures. The model simulates a considerable reduction in precipitation amount until 2025 over most of tropical Africa, amounting to partly more than 500 mm (20–40% of the annual sum), particularly in the Congo Basin and the Sahel Zone. The change is strongest in boreal summer and basically reflects the pattern of maximum vegetation cover during the seasonal cycle. The related change in the surface energy fluxes induces a substantial near-surface warming by up to 7°C. According to the modified temperature gradients over tropical Africa, the summer monsoon circulation intensifies and transports more humid air masses into the southern part of West Africa. This humidifying effect is overcompensated by a remarkable decrease in surface evaporation, leading to the overall drying tendency over most of Africa. Extreme daily rainfall events become stronger in autumn but less intense in spring. Summer and autumn appear to be characterized by more severe

H. Paeth (✉)
Geographical Institute, University of Würzburg, Am Hubland, 97074 Würzburg, Germany
e-mail: Heiko.Paeth@mail.uni-wuerzburg.de

H.-P. Thamm
Geographical Institute, University of Bonn, Bonn, Germany

heat waves over Subsaharan West Africa. In addition, the Tropical Easterly Jet is weakening, leading to enhanced drought conditions in the Sahel Zone. All these results suggest that the local impact of land degradation and reduction of vegetation cover may be more important in tropical Africa than the global radiative heating, at least until 2025. This implies that vegetation protection measures at a national scale may directly lead to a mitigation of the expected negative implications of future climate change in tropical Africa.

1 Introduction

Freshwater availability is the primary factor limiting agriculture and food security in tropical (10°S, 10°N) and subtropical Africa. Therefore, enormous scientific attention has been devoted to the analysis and prediction of the hydrological cycle in this region (e.g. Nicholson et al. 2000; Hulme et al. 2001). These studies were motivated by the frequent occurrence of drought events since the middle of the twentieth century (Nicholson 2001; Le Barbé et al. 2002). Severe droughts were observed in the mid 1970s and 1980s in particular, leading to a general deterioration of living conditions, considerable economic loss and large-scale migration processes (Findley 1994; Benson and Clay 1998). Understanding the mechanisms that cause dry conditions in tropical Africa, is a prerequisite to climate prediction, which in turn is of fundamental importance in agricultural planning and political decision-making and an important challenge for climate modelling efforts (Desanker and Justice 2001; Jenkins et al. 2002). The present study aims to simulate the future climate of Africa up to 2025 under generally realistic assumptions concerning future land use changes and increasing greenhouse-gas (GHG) concentrations. The scenarios utilized are based on a variety of results emerging from previous analyses:

Many studies have shown that atmospheric variability in the low latitudes of Africa is closely tied to changes in the tropical sea surface temperatures (SSTs) (Sutton et al. 2000; Camberlin et al. 2001; Paeth and Friederichs 2004). This is particularly true over Subsaharan West Africa (Ruiz-Barradas et al. 2000) and includes a dipole response between the Sahel Zone (SHZ), spanning the continent from around 12 to 21°N, and the Guinean Coast region (GCR), extending from the coastline along the Gulf of Guinea from 4 to 12°N and to 14°E. A warmer tropical Atlantic Ocean is associated with a more intense north–south gradient in freshwater deficiency (Mo et al. 2001; Paeth and Stuck 2004). Rainfall over coastal East Africa is strongly affected by local and regional SST anomalies in the Indian Ocean (Latif et al. 1999; Black et al. 2003). The relationship between African precipitation and the tropical oceans is embedded in the global teleconnections of the El Niño-Southern Oscillation (ENSO) phenomenon, involving the atmospheric circumglobal Walker circulation (Nicholson et al. 2000; Saravanan and Chang 2000; Janicot et al. 2001).

The northwestern and northern parts of Africa are predominantly influenced by extratropical dynamics including the North Atlantic Oscillation (NAO) and other large-scale modes of the Atlantic-European sector (Cullen and de Menocal 2000; Krichak et al. 2002; Knippertz et al. 2003) as well as SST variations in the northern subtropical Atlantic (Rodriguez-Fonseca and de Castro 2002). The NAO governs the orientation of the North Atlantic storm track and the northeastward extent of the Azores High, which in turn affect temperature and rainfall anomalies in the

Mediterranean basin (Ulbrich and Christoph 1999). Furthermore, Los et al. (2001) and Rowell (2003) point to the role of extratropical SST anomalies in triggering drought conditions in the SHZ.

Although climate model simulations, which are forced by observed SSTs, are able to reproduce the observed phases of positive and negative precipitation anomalies during the twentieth century in tropical Africa, they may nevertheless fail to simulate their amplitudes realistically (Schnitzler et al. 2001; Paeth and Hense 2004). Several authors have suggested that African climate, and rainfall in particular, may be induced primarily by fluctuations in the global SST fields, and secondarily may be enhanced and prolonged by positive feedbacks with land surface properties including vegetation cover and soil moisture (Zeng et al. 1999; Nicholson 2001). Indeed, the climate of the SHZ, which appears to be most sensitive to land degradation (Clark et al. 2001), is also characterized by the longest persistence of rainfall anomalies arising from the memory embedded in vegetation cover and soil moisture (Long et al. 2000). In addition, solar variability may also impose low-frequency variations in African precipitation via changes in the large-scale temperature gradients and atmospheric circulation (Gasse 2001).

A number of papers describe the relationship between land cover changes and the West African monsoon climate. Lotsch et al. (2003) have highlighted the close correlation between observed rainfall amount and vegetation cover in the SHZ. Eklundh and Olsson (2003) report that the slight recovery of rainfall in recent years is associated with an increase in vegetation density as indicated by the NDVI (Normalized Difference Vegetation Index). In addition, the seasonality of rainfall in West Africa has been linked directly to the seasonality of the Leaf Area Index (LAI) (van den Hurk et al. 2003). Modelling studies utilizing atmosphere-land-vegetation models basically confirm that vegetation cover has a primary influence on the shape of the observed African climate zones (Zeng and Neelin 2000; Wang and Eltahir 2000; Zeng et al. 2002; Xue et al. 2004). In general, a reduction in vegetation density leads to a substantial decrease in rainfall amounts over most of tropical Africa (Paeth 2004). Near-surface warming and more intense short-term variability may also be consequences of rediction in vegetation (Bounoua et al. 2000) as well as a shortening of the rainy season and vegetation period, each having negative implications for agriculture and food security (Taylor et al. 2002). Semazzi and Song (2001) have examined the effect of deforestation in the low latitudes of Africa and found the most pronounced drought tendency in the Congo Basin (CGB), which is approximately delimited by the polygon 4°N, 10°S, 30°E and the Atlantic coast. The western Mediterranean region may be affected similarly by deforestation, resulting in reduced evaporation and rainfall (Gaertner et al. 2001).

Soil moisture also plays a major role in the African monsoon climate. In general, high soil moisture levels favour an abundant monsoon (Douville et al. 2001). In addition, soil moisture levels prior to the monsoon season appear to govern the northward extent of humid air masses and the distribution of rainfall (Fontaine et al. 2002). Cook (1999) has suggested a mechanism by which soil moisture may impact indirectly on precipitation via changes in the African Easterly Jet (AEJ). Xue et al. (2004) point to the importance of correct soil moisture initialization in climate models.

There is growing evidence that African climate may also be sensitive to increasing GHG concentrations (Houghton et al. 2001). Although different climate models do

not yet portray a homogeneous picture of the precipitation response to radiative heating (Hulme et al. 2001; Paeth and Hense 2004), it is likely that drier conditions will prevail in the SHZ and CGB as a consequence of increasing GHG concentrations, whereas more abundant rainfall is simulated in the GCR (Clark et al. 2001; Paeth and Stuck 2004). This dipole can be explained physically by a simple linear model of tropical thermodynamics involving a Kelvin and Rossby wave response to an oceanic heat source in the low latitudes (Vizy and Cook 2001). Such a heat source may be characteristic of future climate, when the tropical oceans warm up under the greenhouse (Paeth and Hense 2006). Thus, one of the prominent modes of West African rainfall variability is excited by the greenhouse forcing (Nicholson and Palao 1993), leading to a sharpening of the meridional gradient of freshwater availability in tropical Africa, and possibly to a resulting increase in migration from the SHZ to the GCR (Findley 1994).

From this description of the main influences on African climate as inferred from previous studies, it becomes clear that reliable simulations of future changes in climate, and of the hydrological cycle in particular, have to account for most of these key factors. In particular, the impacts of land degradation and greenhouse forcing need to be evaluated jointly (Douville et al. 2000). Zhao and Pitman (2002) have compared the interactive effects of vegetation loss and radiative heating on annual temperature and precipitation extremes in Europe and China in a set of global climate model sensitivity studies and conclude that the land cover changes contribute considerably to the climate response. Furthermore, Feddema and Freire (2001) have shed light upon the reinforcing effect of soil degradation in global warming experiments. With respect to the African climate, Maynard and Royer (2004a) have shown that the enhanced greenhouse forcing in a global climate model may be a more important factor than land use changes up to the middle of the twenty-first century.

This analysis is linked to the approach of Maynard and Royer (2004a) and presents a number of experiments generating time slices of future African climate until 2025. The basic objective is to provide a regionally differentiated and conceptually sound projection of climate conditions in the near future, that can serve as a basis for planning and political decision-making. For this purpose, the regional climate model REMO (Jacob 2001) is forced using plausible scenarios of vegetation loss, soil degradation, radiative heating, oceanic warming and changes in global atmospheric circulation as simulated by a global climate model. The response patterns for various climate parameters, particularly those associated with the near-surface climate, are presented in order to demonstrate on a step-by-step basis, which physical mechanisms are at work when associating changes in land cover and radiative heating with changes in the hydrological cycle over Africa. A fundamental task within this study is to distinguish between the local and large-scale components of climate response in order to determine the appropriate scopes of action at national and regional levels. A further task is to provide an assessment of climate extremes and their changes up to 2025 as suggested by Trenberth et al. (2003). Any intensification and/or increase in the number of extreme events is presumed to have disastrous socio-economic implications (Changnon 2003; Fowler and Kilsby 2003). Indeed, global climate modelling experiments suggest that climate extremes may become more severe under enhanced greenhouse conditions in most regions of the globe (Meehl et al. 2000; Voss et al. 2002; Kharim and Zwiers 2000). Here, we estimate the extreme value quantiles of daily precipitation and near-surface temperature using the

Generalized Pareto Distribution (GPD) and the methods of L-moments (Hosking 1990). The uncertainty of the extreme value quantile estimates is assessed via a Monte Carlo sampling approach (Kharim and Zwiers 2000). Note that this study is focused on events concering land masses, where the natural and socio-economic systems are most likely to be affected. However, this does not mean that no important changes take place over the oceans.

The study is embedded in the interdisciplinary IMPETUS project on an integrated approach to the efficient management of scarce water resources in West Africa (*I*ntegratives *M*anagement *P*rojekt für einen *E*ffizienten und *T*ragfähigen *U*mgang mit *S*üßwasser in Westafrika, Christoph et al. 2004). Thus, the results of this study are meant to be used in a decision support system for policy makers in West Africa, particularly in Benin and Morocco.

The following two sections provide descriptions of the regional climate model REMO and the experimental design, respectively. The simulated climate changes with respect to various climate parameters are presented in Section 4. The major conclusions of this study are summarized and discussed in Section 5.

2 Model description

The regional climate model REMO is a hydrostatic model designed to simulate atmospheric processes at a synoptic spatio-temporal scale (Jacob 2001). The model equations are based on the operational weather forecast model *Europamodell* previously used by the German Weather Service and have been further developed at the Max Planck Institute for Meteorology (Jacob et al. 2001). The primitive equations are used to compute surface pressure, horizontal wind components, temperature, water vapour and cloud water content as prognostic variables. Physical parameterizations are taken from the global climate model ECHAM4 (Roeckner et al. 1996) and adjusted to the scale of REMO. The mass flux parameterization scheme by Tiedtke (1989) governs the processes of moist convection. A five-layer one-dimensional soil model simulates all processes at the land surface. A more detailed description of the model properties can be found in Jacob et al. (2001) and Paeth et al. (2005).

In the present version, the model is run at 0.5° horizontal resolution with 20 terrain-following vertical levels. The model domain covers the entire tropical and northern parts of Africa from 30°W to 60°E and from 15°S to 45°N. Only this sector is depicted in the following figures. The Mediterranean Basin and the Arabic Peninsula are included as well in order to account for the extratropical impacts in northern Africa. The influence of the atmospheric input data at the lateral boundaries decreases exponentially towards the 8th grid point row of the exterior model region. Thus, REMO can develop its own internal dynamics in this large model area.

REMO can be driven with a range of global atmospheric and oceanic input data. In the uncoupled climate mode, the model is initialized using input data, which are then updated every 6 h only at the lateral and lower boundaries. The atmospheric and oceanic inputs are derived typically from the same global data set. Land surface parameters including vegetation, albedo, orography and etc. are taken from the

GTOPO30 and NOAA (National Oceanic and Atmospheric Administration) data sets, respectively (Hagemann et al. 1999). Some parameters such as vegetation cover, LAI and surface albedo conform to an idealized seasonal cycle. In a previous study (Paeth et al. 2005), a long-term climatology of the late twentieth-century climate was generated with lateral boundary conditions taken from reanalysis data of the ECMWF (European Centre for Medium-Range Weather Forecast, Gibson et al. 1997). This validation study demonstrated that REMO effectively reproduces all major features of the observed African climate. These include the monsoon circulation and tropospheric jetstreams as well as the distribution of temperature, air pressure and precipitation. Even some specific characteristics of the West African monsoon climate, including the bifurcated intertropical convergence zone (ITCZ) and the African Easterly Waves (AEWs) (cf. Hastenrath 2000; Saha and Saha 2001), are simulated realistically. A major deficiency of REMO, typical of regional climate models in tropical Africa (cf. Gallée et al. 2004), is that Subsaharan rainfall is systematically underestimated. This problem is likely related to the coarse grid representation of orography at the Guinean Coast line, which causes the moist convection scheme to be activated off the coast so that fewer humid air masses extend northwards into the West African Subcontinent. Since this underestimation is of systematic nature, it can be corrected using a statistical model. For the purpose of the present study in which difference patterns are emphasized, it is largely irrelevant, assuming that the model bias is linear until 2025.

3 Model experiments

The model experiments described here have been motivated by a number of previous sensitivity studies utilizing the same regional climate model REMO, each one addressing a single isolated key factor influencing African climate (Paeth 2004; Paeth and Stuck 2004). Figure 1 displays the changes in annual rainfall up to 2025 due

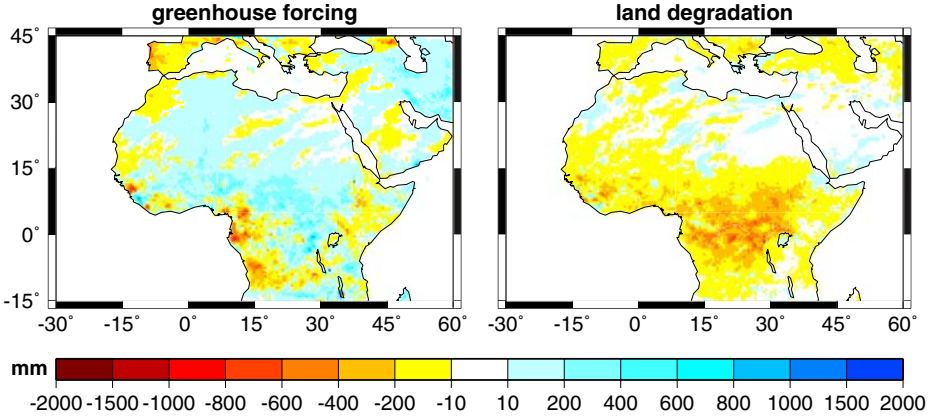

Fig. 1 Changes in total annual precipitation around 2025 in mm due to enhanced GHG concentrations (*left*) and ongoing land degradation (*right*)

to enhanced greenhouse conditions (left) consistent with IPCC SRES scenario B2 (Nakicenovic et al. 2000), and land degradation (right) corresponding to a decrease of 25% over entire tropical Africa, which is roughly equivalent to the land use scenario described below. With the exception of some minor areas along the Guinean Coast and particularly in the western CGB, the increased radiative forcing leads to more humid conditions (cf. Houghton et al. 2001). In contrast, reduced vegetation cover and soil degradation are associated with a substantial reduction in annual precipitation over the SHZ, GCR and in particular, the CGB. By comparing the two response patterns and assuming a linear interaction between the two forcings, the following a-priori hypotheses can be proposed: In the GCR, the rainfall reduction due to vegetation loss and soil degradation may be more than offset by stronger moisture convergence due to GHG-induced oceanic heating (cf. Clark et al. 2001; Vizy and Cook 2001). The increased radiative forcing is less influential in the SHZ, where land degradation may cause a substantial decrease in precipitation, especially given the presently low annual rainfall of less than 200 mm (Saha and Saha 2001; Paeth et al. 2005). In most of the CGB, both forcings cause dryer conditions as a regional mean. In order to assess the likely nonlinear interactions between different forcings and to provide realistic simulations of future African climate, in this study the REMO experiments incorporate all of these forcings simultaneously. A range of time slice experiments were conducted, embodying estimates of land use changes and increasing GHG concentrations up to 2025.

Each time slice experiment covers one year with forcing conditions corresponding to the years 2000, 2005, 2010, 2015, 2020 and 2025. The fact that no simulations are made beyond 2025 reflects the scope of the IMPETUS project, which aims at providing decision support for policy makers at most two decades into the future. Each scenario run is subject to five simultaneous forcings: (1) Atmospheric fields from a global coupled climate model simulation with ECHAM4/HOPE (Roeckner et al. 1996) provide the lateral boundary conditions. These data cover the period 1860–2100 and are forced by enhanced GHG concentrations according to IPCC scenario SRES B2 (Nakicenovic et al. 2000). The choice of emission scenarios is rather arbitrary since very little difference is found between the various SRES scenarios until 2025, at least with respect to the primary factors defining African climate. (2) An identical GHG increase is imposed within REMO, which modifies the radiation budget within the model domain. (3) The oceanic lower boundary conditions are also taken from the global ECHAM4/HOPE run. In order to eliminate a part of the interannual variability, which may partly mask the transient climate changes, the SST fields are smoothed by a 5-year lowpass filter. This ensures that the ocean surfaces, which are supposed to be a key factor influencing the African monsoon climate (Nicholson 2001; Paeth et al. 2005; Paeth and Stuck 2004), are continuously warming from time slice to time slice. Note that the resulting slight inconsistency between lower and lateral boundary conditions does not lead to noticeable nonconformities in the simulated regional climate (cf. Paeth and Hense 2006).

(4) The scenarios of future vegetation loss reflect estimates by the United Nations (www.gisdevelopment.net/aars/acrs/1997/ts12/ts12003pf.htm) and were derived from the observed relationship between global vegetation cover and population density during the last decades. Changes in vegetation cover as derived from NOAA satellite data were associated with population density revealing a close correlation, ranging from 0.71 to 0.91 for various regions of the globe (Pahari and Murai 1997). Estimated

population growth up to 2025 was provided by CIESIN (1996). Using this approach, the deforestation rate for tropical Africa was predicted to be 1.06% per year during the 1990–2025 period. These estimated trends are backed up by IPCC (Houghton et al. 2001) and UNEP (2003). Unfortunately, the estimates consist only of individual values taken as representative of an entire region – for instance a reduction of 32% over the entire SHZ through 2025. To be suitable for use in REMO, these estimates had to be transformed to a spatial grid-box pattern, while reflecting that the land use changes are not fully homogeneous in space. For this purpose, the West African subcontinent has been divided into several primary regions. Within each region, spatially heterogeneous vegetation changes have been assigned randomly for each grid box, subject to the condition that the regional mean sums up to the UN estimates exactly. Some additonal assumptions were used to construct the forcing patterns, for example that the vegetation loss is more (less) pronounced in the transition zone between Sahara and Sahel (in the inner core of the tropical rain forests). The resulting patterns of the vegetation ratio for present-day and 2025 are displayed in Fig. 2 (left panels). With respect to 2000, a heteroneous pattern of vegetation reduction occurs in 2025 with largest amplitude in tropical Africa. Some minor changes are also imposed in northern, eastern and southern Africa as well as over the Arabic Peninsula. According to the UN estimates, Europe is barely affected by land use changes up to 2025. For the remaining time slice experiments between 2000 and 2025, the 2025 minus 2000 difference pattern of the vegetation ratio has been linearly interpolated. In addition to the vegetation ratio, there are other surface parameters in REMO, which are linked to changes in vegetation cover. These are LAI, forest fraction, roughness length and surface albedo. Maynard and

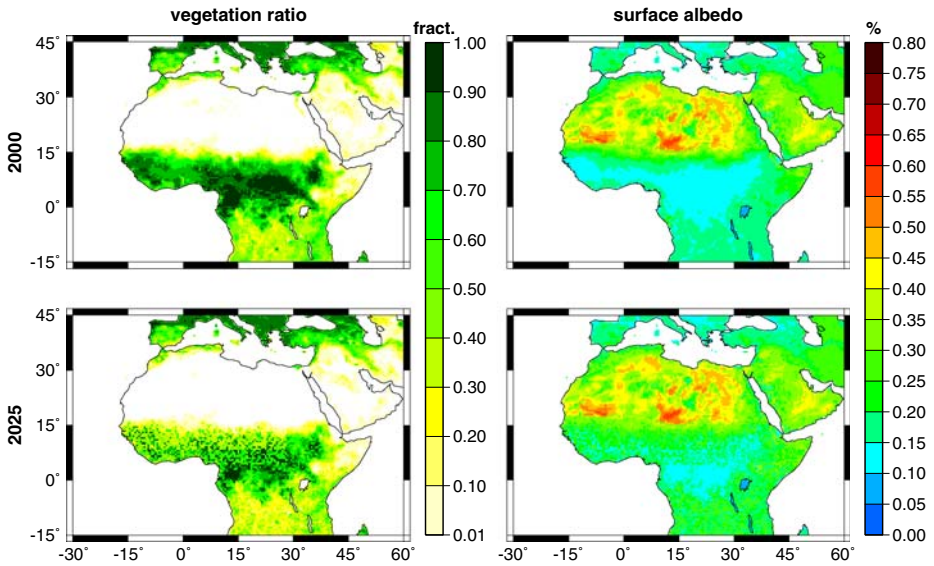

Fig. 2 Prescribed quasi-realistic vegetation scenarios: examplary patterns of vegetation ratio (*left*) and surface albedo (*right*) 2000 and 2025

Royer (2004b) have shown that none of these surface parameters dominates the others, rather all of them have to be taken into consideration equally when simulating vegetation changes (cf. Paeth 2004). With the exception of albedo, the other surface parameters are modified in the same way as the vegetation ratio. However, surface albedo is a function of LAI, forest fraction and vegetation ratio. Therefore, a multiple linear regression analysis encompassing all grid boxes was applied to construct the forcing patterns of surface albedo in Fig. 2 (right panels). As anticipated, albedo increases wherever the vegetation cover is reduced. The increase amounts to 15%, implying a remarkable modification of the energy balance at the surface. We do not claim that the patterns in Fig. 2 are entirely realistic in every detail. It is difficult in practice to predict the $0.5^\circ \times 0.5^\circ$ grid boxes, in which human activity will cause the strongest land degradation through 2025. However, it is likely that future land use changes may possess the same extent of heterogeneity as the random patterns depicted in Fig. 2, with some subregions being more affected than others. Therefore, we assume that the prescribed forcing patterns utilized are reasonable, provided that the UN estimates are realistic.

(5) Modification of the vegetation-related surface parameters as described above has a direct impact on the soil processes in REMO: changes in soil temperature and soil hydrology are induced as well. This holds particularly for soil moisture, which has an important impact on the West African monsoon climate (Douville et al. 2001; Fontaine et al. 2002). However, there are numerous soil parameters in REMO, that are usually held constant over the entire integration period. These soil parameters govern the ratio between infiltration and evaporation on the one hand and surface runoff and drainage on the other hand. It is likely that this ratio will change towards more lateral runoff/drainage and less infiltration/evaporation under a scenario of soil degradation (Feddema and Freire 2001). Therefore, a continuous modification of the soil parameters is imposed from time slice to time slice, resulting in weak soil degradation by 2025. In addition, the wilt point has been increased, leading to a reduction in soil water available to plants and hence to transpiration. Unfortunately, the modification of the soil parameters cannot validated by empirical data or measurements. Given this uncertainty, we have chosen a scenario of rather modest soil degradation in order to avoid an overestimation of the climate response. In a previous sensitivity study using REMO, the isolated effect of soil degradation was found to be considerably less pronounced than the isolated impact of reduced vegetation cover, yet tending in the same direction (Paeth 2004).

This description indicates that the time slice experiments are subject to a complex combination of forcing scenarios, which are intended to provide a reasonably realistic simulation of future African climate. However, there is still some uncertainty in this experimental design: while most forcings (vegetation and soil degradation, GHG concentrations and oceanic warming) are linearly or at least continuously enhanced from time slice to time slice, the atmospheric input data from ECHAM4/HOPE are characterized by interannual variability. This implies that the selected time slices are not necessarily representative of the expected transient climate change trends. Therefore, results are only plotted if the long-term linear trends between 2000 and 2025 are statistically significant at the 10% level. As described above, shorter-term interannual fluctuations arise from the atmospheric forcing data provided by the global model. Given the small number of degrees of freedom over six time slice

experiments, this is quite a conservative measure of the long-term trends in African climate. As a consequence, if a trend is not plotted in a grid box it means either that there is no change or that the long-term change is obscured by strong interannual fluctuations.

4 Results

4.1 Precipitation

Since freshwater from precipitation is a key factor in West African agriculture and food security, we begin by presenting the simulated changes in total annual rainfall (Fig. 3). The present-day annual rainfall pattern exemplifies the typical meridional gradients in precipitation amount with a minimum in the inner Sahara (<50 mm) and a maximum in the inner tropics (up to 2,000 mm) (not shown, see (Saha and Saha 2001; Paeth et al. 2005) or many other papers, text books and atlases). Intermediate rainfall accumulations are simulated for coastal northwestern African. The pattern simulated by REMO is broadly realistic with a slight underestimation over subsahelian West Africa and is in good agreement with a previous REMO experiment driven by the more realistic reanalysis data (Paeth et al. 2005). At first glance, annual precipitation amount is substantially reduced in 2025, especially in tropical Africa (bottom left). The remaining patterns (to the left) indicate the respective differences between each future time slice and 2000. In general, there is a progressive reduction in rainfall from 2000 until 2025. However, some regions, such as parts of the Guinea Coast and the western Sahel, may experience more humid conditions. Other parts of Africa, such as central northern Africa, are characterized by strong interannual variations. This is also indicated in the bottom four (right) panels showing the relative differences between time slices. In the case of a strictly linear response in African rainfall these patterns would be identical. This is obviously not the case, but rather that long-term trends are overlaid by shorter-term variations imposed by the ECHAM4 atmospheric input data at the lateral boundaries. Therefore, the linear trend pattern (top right) does not reveal statistically significant changes at all grid points as suggested by the difference pattern 2025 minus 2000 (bottom left). The negative trends are significant in large parts of tropical Africa with highest amplitudes in the CGB and southern SHZ. Some positive anomalies are simulated over the western Sahara. The positive trends over the central GCR are barely significant. Note that it is likely that more significant trends would be identified if a larger number of time slices was available, rising the number of degrees of freedom. However, the trend pattern clearly demonstrates that anticipated future land degradation and greenhouse warming will probably be associated with much dryer conditions in most of tropical Africa, except for some regions of the Guinean Coast. Furthermore, the trend pattern is very similar to the rainfall response induced by vegetation changes alone as shown in Fig. 1. This may be indicative of the dominating impact of land use changes in African climate change at least until 2025, during which time the GHG signal is still not too overwhelming.

Since most regions in Africa are characterized by a well-defined rainy season, it is of interest to distinguish between respective seasonal changes in precipitation

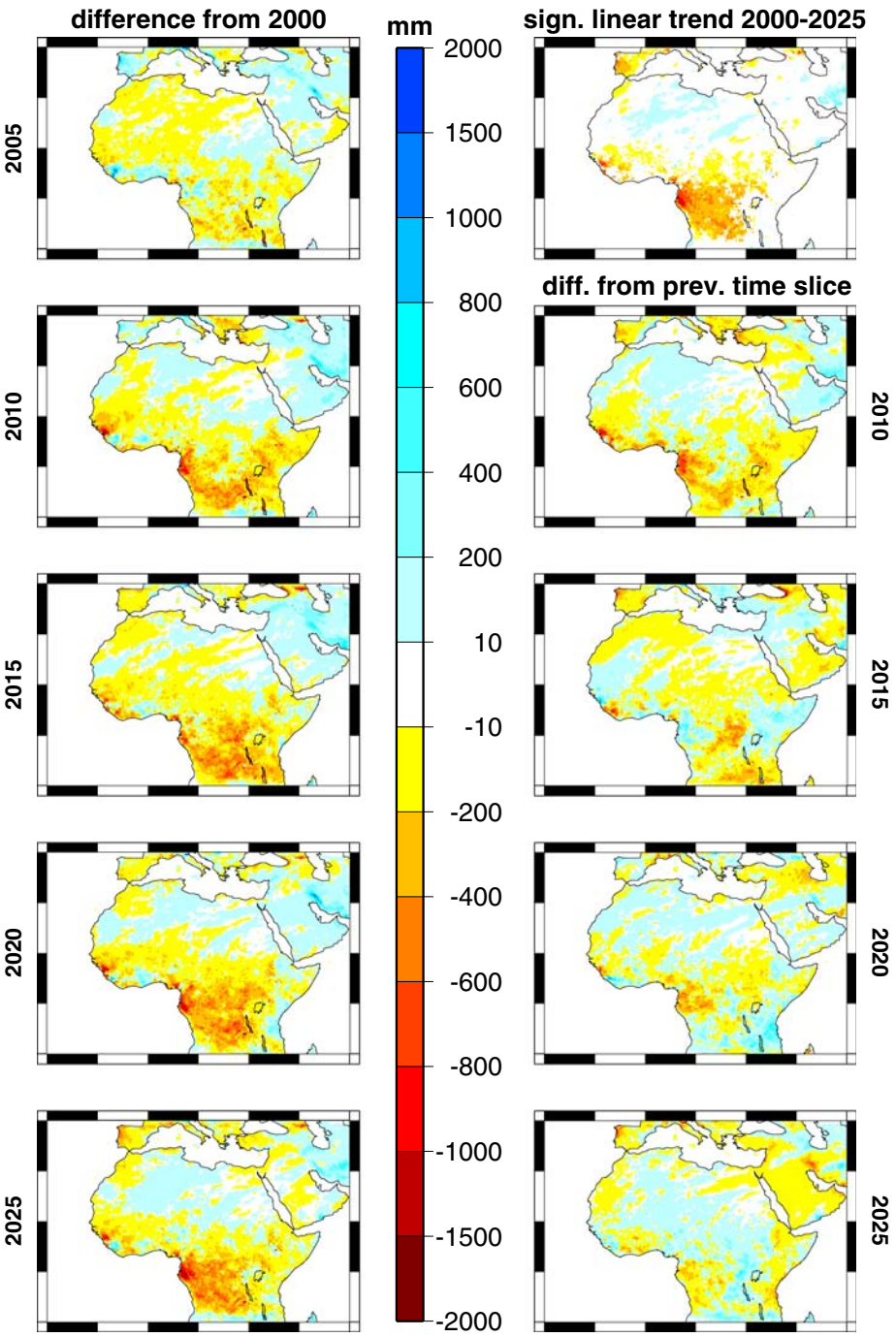

Fig. 3 Changes in total annual precipitation in mm due to the combined forcing: differences from 2000 (*left panels*), differences from previous time slice (*right panels*), and linear trend pattern 2000–2025 (*top right*). Trends are only plotted, if the 10% significance level is exceeded

(not shown). In boreal winter (December-February, DJF), which corresponds with the dry season in tropical West Africa but with the wet season in northwestern and southern Africa, rainfall is less sensitive to the imposed forcings than in the remaining seasons. There are some negative trends in the inner tropics, particularly in the southern CGB. In spring (March–May, MAM) and summer (June–August, JJA), most of tropical Africa experiences a dryer climate up to 2025. The southern SHZ in particular seems to be affected by land degradation and/or radiative forcing, resulting in a weaker or later beginning of the rainy season in spring. Surprisingly, more precipitation is simulated during autumn (September–November, SON) over West Africa, but the CGB is still subject to dryer conditions. The patterns of seasonal rainfall response are highly reflective of the distribution of vegetation and the solar maximum throughout the seasonal cycle and point to the importance of land cover changes with respect to vegetation cover and surface albedo.

The question of whether the impacts of the "treatments," land degradation and enhanced greenhouse warming, are statistically significant given the high level of internal rainfall variability can also be evaluated. This issue can be addressed by one-way analysis of variance (ANOVA), used to distinguish between the externally induced mean changes up to 2025 and the day-to-day fluctuations of precipitation (von Storch and Zwiers 1999). The fraction of variance explained by the external forcings is plotted in Fig. 4. The signal does not stand out from the interseasonal variability during the whole year (not shown). This is not surprising, given the sharp contrast between wet and dry seasons, implying stronger rainfall changes within the

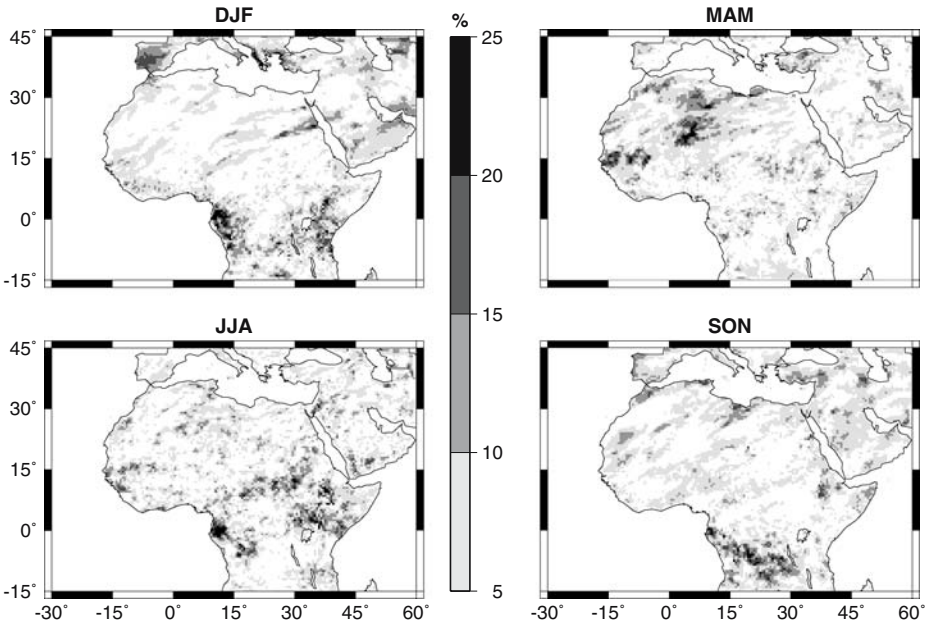

Fig. 4 Portion of total 5-day variance in % explained by the combined forcing, as inferred from analysis of variance. Values are only plotted, if the 1% significance level is reached

seasonal cycle than between 2000 and 2025. At an intraseasonal time scale, however, the long-term rainfall changes are statistically significant and account for up to 25% of total variability in several regions, although the patterns are quite heterogeneous in space. The signal is slightly more pronounced in the tropics, where the day-to-day variations are minor. There is no obvious difference between the individual seasons, except for a spatially somewhat more coherent signal in Northern Hemisphere spring and summer. Albeit statistically significant at the 1% level, the forcings generally account for a small fraction of variance. This is due to the high amount of internal rainfall variability in tropical and subtropical Africa and confirms that precipitation is a very noisy variable for detecting climate change, especially at short time scales (cf. Paeth and Hense 2002).

In order to learn, which of the impact factors – land degradation or greenhouse warming – is more relevant to African climate change up to 2025, we must first understand the physical mechanisms, which lead to the overall reductions in precipitation. For this purpose, it is distinguished between the more local and more regional responses of African climate. In terms of rainfall, this implies distinction between convective and large-scale precipitation. Both contribute to the total rainfall rates in REMO, whereas the convective component generally dominates in the low latitudes, particularly outside the central monsoon regions. Figure 5 clearly indicates that convective annual rainfall is affected more extensively by the combined forcings than is the large-scale component. Negative trends are statistically significant over most of tropical Africa. With respect to large-scale precipitation, the trend pattern is much more disperse, but positive anomalies prevail over some parts of tropical West Africa and the inner Sahara. Note that the response of convective precipitation in particular may differ from model to model depending on the parameterization scheme. The following is a step-by-step description of how this contrasting behaviour of convective and large-scale precipitation arises from the overall climate response, involving the more localized energy balance and the large-scale atmospheric circulation.

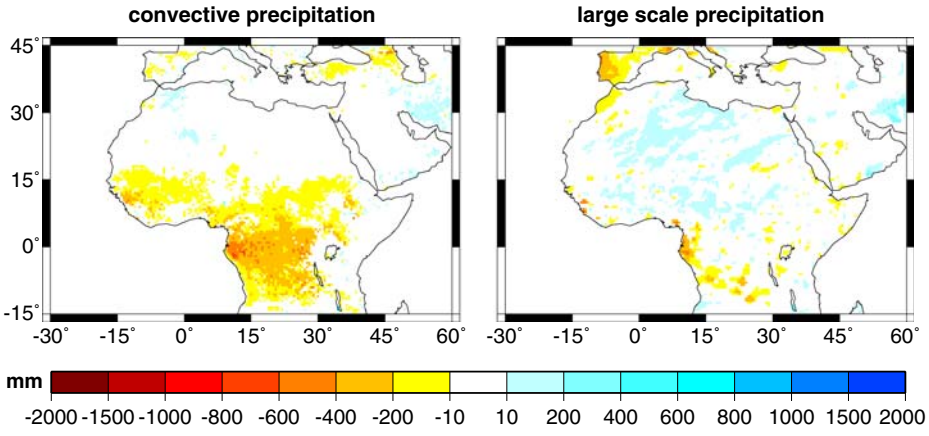

Fig. 5 Changes in convective (*left*) and large-scale (*right*) annual precipitation in mm: linear trend pattern 2000–2025. Trends are only plotted, if the 10% significance level is reached

4.2 Near-surface energy balance

There is a prominent interaction between changes in precipitation and thermal anomalies near the Earth's surface. On the one hand, rainfall and cloud cover affect the radiation balance and temperature at the ground. On the other hand, precipitation is influenced by soil moisture, evaporation and atmospheric circulation. The seasonal trend patterns of 2 m temperature are shown in Fig. 6. Land degradation and greenhouse forcing are accompanied by a general warming in the entire model domain. However, the changes are only significant in the lower latitudes. In tropical Africa, near-surface temperature may locally rise by up to 5°C by 2025. In most grid boxes 2–4°C are simulated. This warming rate is extreme and of the same order of magnitude as most IPCC estimates of GHG-induced global warming through the end of the twenty-first century (Houghton et al. 2001). As with precipitation, the temperature changes during DJF appear to be confined to a smaller part of the continent than during the other seasons. The patterns appear to reflect the occurrence of high vegetation density in the seasonal cycle, as was observed for the seasonal rainfall changes. This suggests that until 2025, land cover changes are more influential on near-surface heating in Africa than is radiative forcing. This interpretation is supported by the observation that almost no significant temperature trends are simulated in the extratropics, although the same increase in GHG concentrations is imposed everywhere in the model region. Another explanation may reflect a change in extratropical circulation in the global climate model (Ulbrich and Christoph 1999), involving a positive trend of the NAO, which in turn causes negative

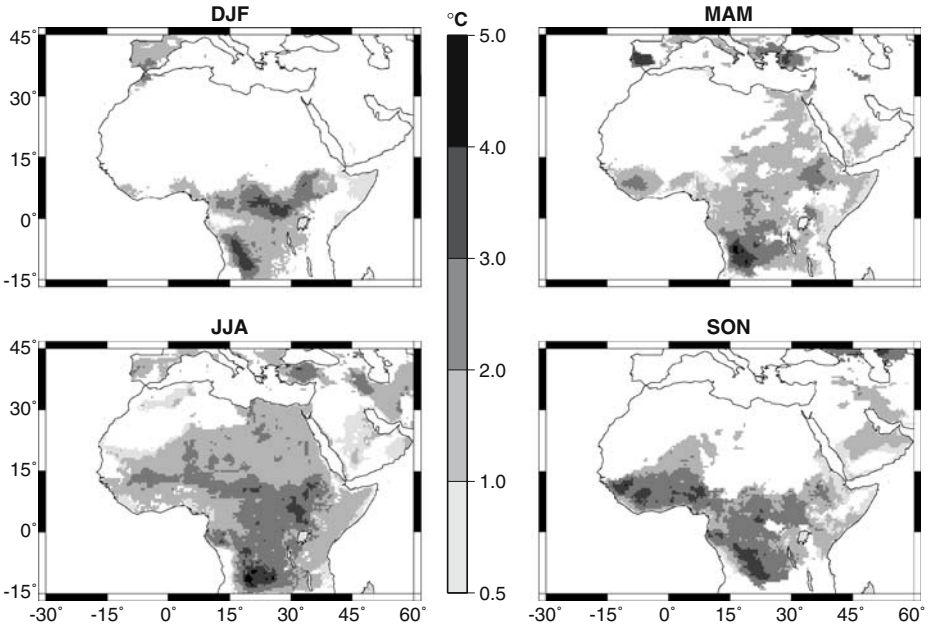

Fig. 6 Changes in seasonal-mean near-surface temperature in °C: linear trend pattern 2000–2025. Trends are only plotted, if the 10% significance level is reached

temperature anomalies in the Mediterranean Basin (Cullen and de Menocal 2000) and may compensate the radiative heating.

We now approach the question as to how land degradation results in this striking warming at the ground level. A direct link is provided by the heat fluxes at the surface: a reduction in vegetation cover is associated with less transpiration and interception as well as decreasing soil moisture. The modification of the soil parameters also induces a reduction in soil moisture and evaporation. In addition, the increased wilt point inhibits transpiration by plants. Finally, less rainfall leads to less soil moisture and evaporation. Thus, a substantial decline in latent heat fluxes from the land surface into the atmosphere is expected. Figure 7 basically supports this hypothesis. The reduction in surface evaporation is even of the same order of magnitude as the climatological values, indicating a remarkable dehydration of the soils. The seasonal patterns are again similar to the annual cycle of vegetation cover, solar maximum and related changes in precipitation (Fig. 3) and temperature (Fig. 6). There appears to be a direct local relationship between land degradation on the one hand and a shift of the Bowen ratio, which denotes the ratio between sensible and latent heat fluxes from the surface into the atmosphere, towards greater sensible heat fluxes, strong surface heating and diminished rainfall amount on the other hand. Theoretically, the positive temperature trends due to increased sensible heat fluxes may be somewhat counterbalanced by weaker turbulent exchanges in the atmospheric boundary layer, since surface roughness decreases with vegetation loss. However, the Bowen ratio seems to embody the primary mechanism. In addition, it will be shown in Section 4.3 that simulated wind speed is increasing which in turn implies enhanced turbulent exchanges. Thus far, all results and physical interpretations highlight the crucial role

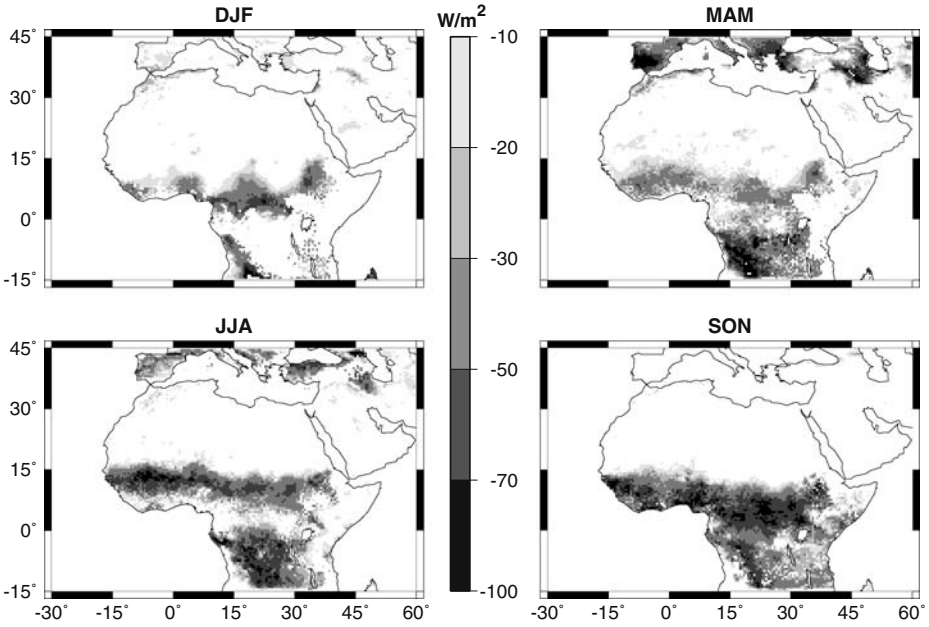

Fig. 7 Same as Fig. 6 but for latent heat flux from the surface in $\frac{W}{m^2}$

of land use changes in future African climate change at a local scale. Furthermore, it is likely that the lower-tropospheric warming is accompanied by a modification of atmospheric circulation, particularly in the West African monsoon system, which is governed by large-scale temperature gradients (Saha and Saha 2001).

4.3 Atmospheric circulation

The simulated near-surface wind fields over tropical Africa are characterized by the typical monsoon flow rotation from winter to summer (Fig. 8, top panels). In boreal winter (DJF), dry northeasterlies, known as Harmattan winds, prevail over most of the West African subcontinent and largely inhibit cloud and precipitation processes during the dry season. In JJA, the Subsaharan region of West Africa is under the influence of humid air masses from the tropical Atlantic, leading to a rainfall maximum at around 10°N (Saha and Saha 2001). The mean wind vectors also reflect the seasonal position of the ITCZ which extends northward from 6°N in winter to 20°N in summer. Northwest Africa is within the influence of the Azores High, which is more pronounced and more shifted towards the central subtropical North Atlantic in winter. East Africa is also subject to seasonally rotating wind directions although the contrast between the associated air masses is less distinct than in West Africa. In the combined forcing scenario, wind speed is increasing over tropical West Africa, particularly in JJA (not shown). This is consistent with

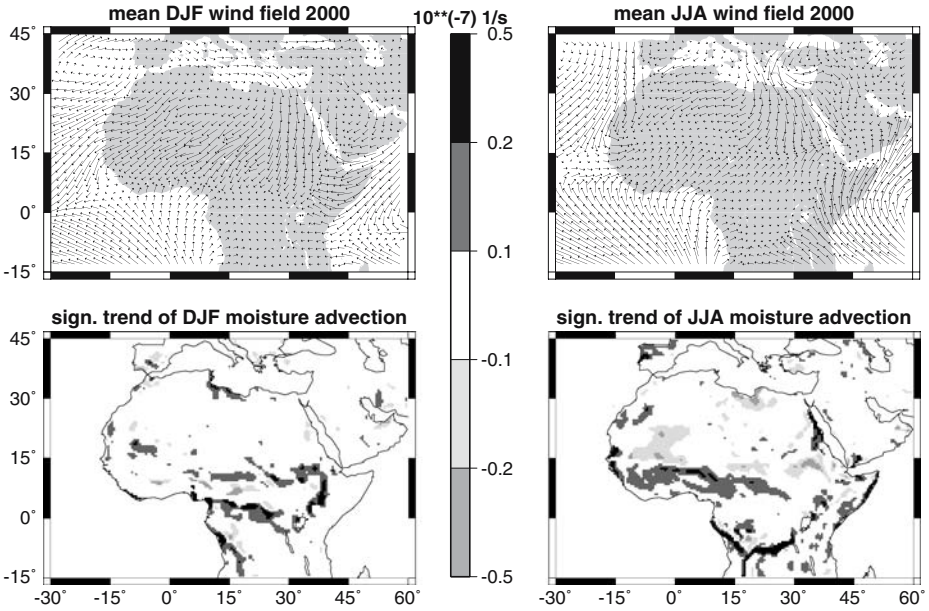

Fig. 8 Mean patterns (2000) of DJF and JJA near-surface wind in $\frac{m}{s}$ (*top*). Linear trend patterns 2000–2025 of DJF and JJA near-surface moisture advection in $10^{-7}s^{-1}$ (*bottom*). Positive changes imply a flow-related increase in moisture in a given grid box. Trends are only plotted, if the 10% significance level is reached

the expectation of an accelerated summer monsoon flow into the regions of highest surface heating in Subsaharan Africa. At the same time, the southeasterly winds over coastal East Africa become weaker. The wintertime Harmattan is barely affected until 2025. The only striking signal in DJF is the enhanced flow into the heat source in western tropical Africa as shown in Fig. 6. No spatially coherent changes are found in the extratropics, probably because extratropical circulation in the global ECHAM4 model does not respond significantly to the greenhouse forcing until 2025 (cf. Ulbrich and Christoph 1999; Rauthe et al. 2004).

Advection of moist air into an imaginary atmospheric column is an important process in the generation of rainfall. Moisture advection is closely tied to the convergence and divergence of the wind field and to the spatial gradients in specific humidity. In DJF, moist air is transported primarily into the southernmost part of West Africa and into tropical East Africa where the ITCZ is located. During the summer monsoon circulation a broad zone of maximum moisture advection extends far north into the SHZ. The bottom panels in Fig. 8 depict the significant linear trends in DJF and JJA moisture advection until 2025. Land degradation and radiative heating scarcely impact on the wintertime moisture advection. In JJA, the zone of maximum moisture enrichment is shifted towards the Guinean Coast. This is related to a southward shift of the ITCZ and is consistent with the linear theory of atmospheric response to a tropical heat source (Paeth and Hense 2006; Vizy and Cook 2001): In the context of oceanic heating in the tropical Atlantic, the ITCZ undergoes a southward displacement with positive (negative) rainfall anomalies in the GCR (SHZ). Thus, the change in JJA moisture advection may be interpreted as an indicator of GHG-induced oceanic warming. In general, positive anomalies of moisture enrichment are supposed to favour abundant rainfall. This large-scale effect appears to be overcompensated by local changes in evapotranspiration, since total precipitation is reduced over tropical Africa (Figs. 3 and 7). The discrepancy between the responses of convective and large-scale precipitation (Fig. 5) can now also be explained: the modified summer monsoon circulation produces more large-scale rainfall, whereas the remarkbale reduction in evaporation over the land masses inhibits the processes of moist convection at the local scale. This finding may have high political relevance, as will be discussed in Section 5.

The West African monsoon system and the distribution of rainfall are directly linked to middle and upper tropospheric circulation (Saha and Saha 2001). In particular, the AEJ (Cook 1999) and Tropical Easterly Jet (TEJ) (Hastenrath 2000) influence the occurrence of droughts in the SHZ. The TEJ can be illustrated by the JJA wind field at 200 hPa (Fig. 9): Easterly winds prevail in a broad zone between 6 and 20°N, surrounded by the subtropical jetstream to the north and intertropical westerlies to the south. In a warmer climate, the TEJ is simulated as becoming much weaker. The westerlies over the equator intensify to the same extent. In general, a weaker TEJ is connected to drought conditions in the SHZ because it is dynamically linked to the AEJ and AEWs, which are responsible for a large portion of the total rainfall amount in subsaharan Africa (Hastenrath 2000). Thus, an additional factor in rainfall reduction over tropical Africa may arise from changes in the large-scale tropospheric circulation. Since the dynamics of the TEJ are mainly established at the eastern boundary of the REMO domain, it is likely that the global climate model ECHAM4/HOPE already contains a climate change signal in the upper-tropospheric flow of the low latitudes.

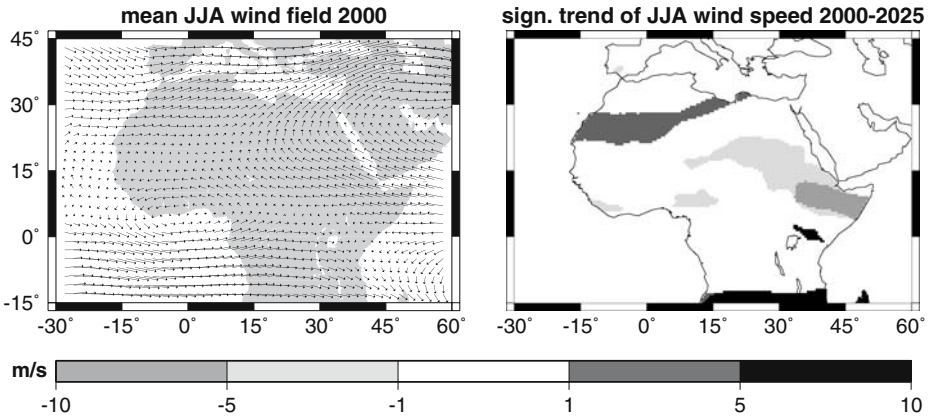

Fig. 9 Mean pattern (2000) and linear trend pattern (2000–2025) of JJA wind in 200 hPa in $\frac{m}{s}$. Trends are only plotted, if the 10% significance level is reached

This result is a further indication that future climate changes in Africa are embedded in a variety of phenomena and processes in the climate system at different spatial and temporal scales, which all need to be represented correctly in the simulations. It also points to a general problem with the experimental setup used here: The dynamics in REMO are partly driven by the local changes in land cover and partly by flow anomalies and climate change signals imposed by the global climate model, which itself is not aware of the land cover changes. This may lead to some inconsistencies which can only be dealt with when using global input from models with similar land use scenarios. This is planned in the next step. In terms of the monsoon and moisture advection changes in the heart of the REMO domain (Fig. 8), the results can be attributed coherently to the local land cover changes. However, with respect to the AEJ changes at the eastern boundary of REMO (Fig. 9), it is conceivable that this signal is emanating from the global climate model. Thus, global circulation is also an important player in African climate change in addition to local changes in land cover and greenhouse-gas concentrations.

4.4 Climate extremes

Thus far simulated changes in the mean state of African climate have been presented. A further important question is the extent to which climate extreme events are affected by global warming and land degradation, since changes in climate extremes are anticipated to have even more severe socio-economic implications than general warming or drought tendencies (Changnon 2003; Fowler and Kilsby 2003; Trenberth et al. 2003). However, the estimation of climate extremes is less than straightforward given the fact that they are by definition infrequently observed (Palmer and Räisänen 2002): An appropriate statistical distribution must be identified and fitted to a sufficiently large sample of extreme events in order to obtain a reliable estimate of the climatic behaviour in the upper tails of the distribution (Meehl et al. 2000; Palmer and Räisänen 2002). In addition, the level of uncertainty associated with the extreme value estimates must be quantified when interpreting the results (Kharim and Zwiers

2000; Park et al. 2001). Here, we fit the Generalized Pareto Distribution (GPD) to seasonal daily precipitation and near-surface temperature above a chosen threshold, varying between the 85 and 95% quantiles. The three parameters of the GPD are determined by the method of L-moments and the return values (RVs) corresponding to various return times $T \epsilon [1, 5, 10, 20, 50, 100]$ years are extrapolated from the fitted distribution for each time slice individually (Hosking 1990). The reliability of the RV estimate at different return time T is evaluated by a bootstrap sampling approach, producing 1,000 artificial samples and corresponding RV estimates (Kharim and Zwiers 2000). Park et al. (2001) have demonstrated that such RVs are normally distributed over a sufficiently large number of bootstrap samples. Thus, the standard deviation of the sample RVs over the 1,000 samples is a measure of the standard error of the extreme value estimate, which can then be used to construct a confidence interval around the mean RV estimate. The resulting signal-to-noise ratio of the RV estimate is only reasonably high for the 1-year RVs (not shown). Therefore, this analysis is restricted to these relatively short-term climate extremes. In the following figures the 1-year RVs are shown for those thresholds $q \epsilon [85..95]$ %, which are associated with the smallest standard error or highest reliability. This methodology is applied to the GCR and southern SHZ only, where the largest simulated changes in the mean hydrological cycle have been observed (see Sections 4.1 and 4.2). In order to enlarge the sample size, four grid boxes are pooled, when fitting the GPD and calculating the RVs. Therefore, the resolution is reduced by a factor of two in the following figures.

The seasonal and spatial distribution of present-day extreme values as estimated from the 2000 time slice is depicted in Fig. 10a,b. With regard to daily rainfall, the most severe daily extremes, which usually occur once a year, are simulated in Northern Hemisphere spring and summer over the tropical Atlantic off Liberia and in the vicinity of the Guinean mountains, amounting to up to 600 mm (Fig. 10a). There is a general north-south gradient in the occurrence of strong extremes with maxima in JJA over the ocean and minima in DJF over the southern SHZ. In JJA, when the ITCZ extents far north and the rainfall maximum penetrates into the Sudan Zone and southern Sahel, heavy rainfall events of 100–300 mm/day are also simulated in this region. In DJF, when the ITCZ resides over the Guinea Coast, no rain rate above 30 mm a day is found over the continent. Note that these simulated extreme values have to be interpreted with care from a quantitative point of view. It is well-known that climate models tend to underestimate the strongest observed precipitation extremes, while producing an oversized number of weak rainfall events (Zolina et al. 2004). Assuming that this deficiency is of systematic nature, the difference patterns in Fig. 11a,b should be more reliable. Unfortunately, there is no daily observational data set in this region, which is sufficiently complete and extended in time, to validate the regional climate model output for a simulation period in the past.

The patterns of 2 m temperature extremes basically reflect the seasonal cycle of the solar maximum and the position of the ITCZ with enhanced cloud cover (Fig. 10b). The picture is practically an inverse of the rainfall extremes in Fig. 10a with minima of about 26°C in the upwelling regions of the tropical Atlantic and maxima in MAM and JJA over the SHZ, amounting to almost 44°C in the daily mean. Towards the Guinean Coast, where cloud cover, precipitation and soil moisture are larger, the heat waves are much less pronounced, not exceeding 34°C.

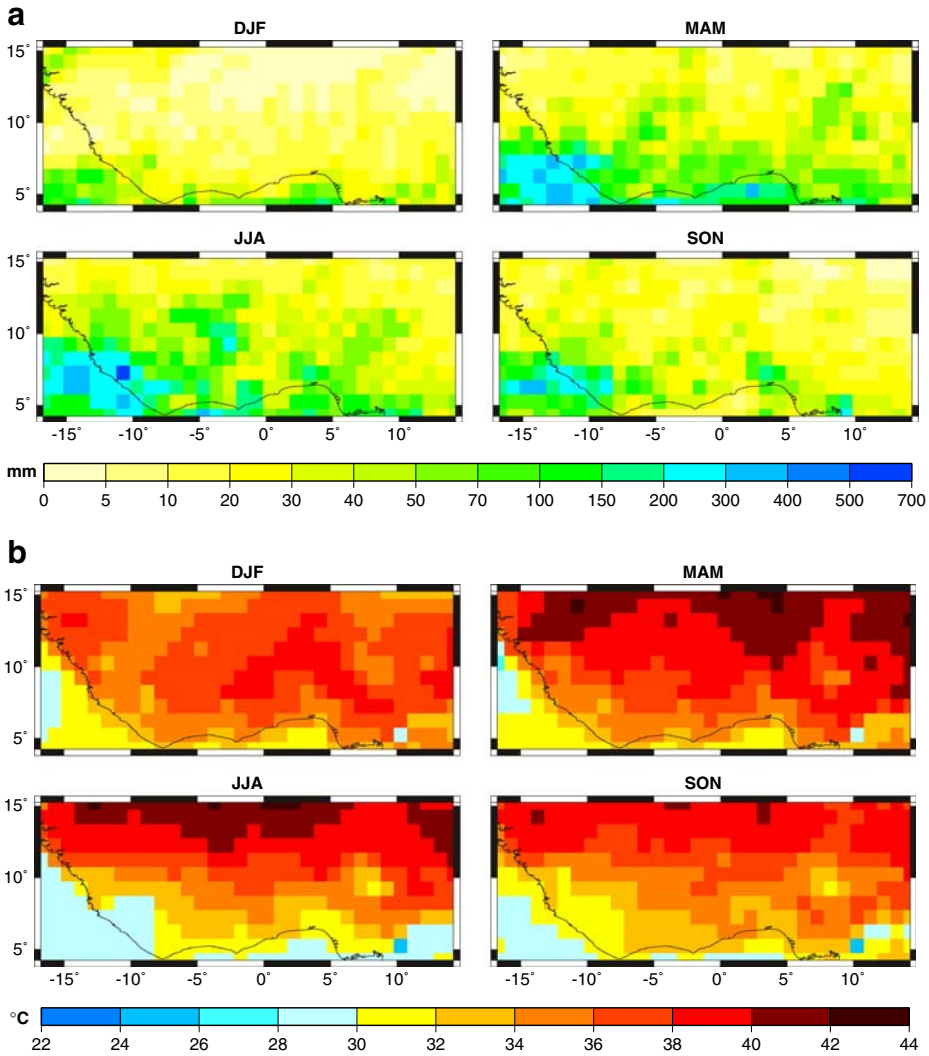

Fig. 10 **a** One-year return values of seasonal extreme daily precipitation in 2000 in mm, tropical West Africa. **b** Same as Fig. 10a but for daily near-surface temperature in °C, tropical West Africa

When considering the changes in climate extremes between 2000 and 2025, it is is a clear requirement that the corresponding level of significance be estimated, since the RV estimate is subject to large uncertainty and data samples drawn from differing periods will likely lead to different extreme value estimates (Kharim and Zwiers 2000). In the present study, we evaluate the significance of changes in RVs in the following way: (1) 1,000 RV estimates are derived from the bootstrap samples separately for the time slices 2000 and 2025. (2) Assuming normal distribution of estimated RVs (Park et al. 2001), the 90% confidence intervals for the 1,000 RVs are estimated for 2000 and 2025. (3) Changes in extreme values are only plotted if the

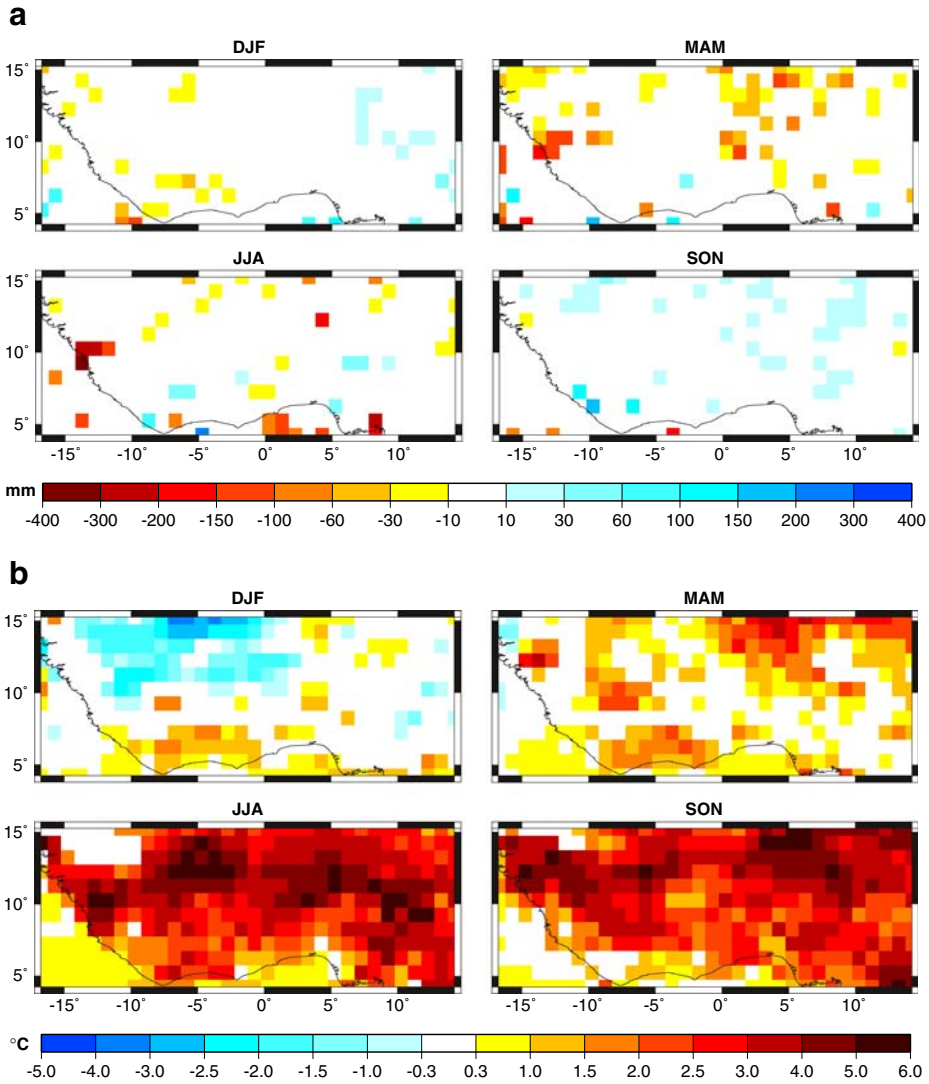

Fig. 11 **a** Changes in 1-year return values of seasonal extreme daily precipitation 2000–2025 in mm, tropical West Africa. Only values are plotted where the change is statistically significant at the 1% level as inferred from the 1,000 bootstrap samples. **b** Same as Fig. 11a but for daily near-surface temperature in °C

90% confidence intervals of the 2000 and 2025 RVs do not overlap, being equivalent to the 1% significance level of the RV changes. For daily precipitation extremes, a heterogeneous picture is presented (Fig. 11a) (cf. Bell et al. 2004): While most seasons and grid boxes are characterized by less severe rainfall events by 2025, in autumn maxima appear to increase by more than 100 mm/day in the western GCR, but only in individual grid boxes. In general, only a small number of grid boxes is subject to statistically significant changes in rainfall extremes. This is due to the

high level of uncertainty in the RV estimate. Compared with the mean changes depicted in Fig. 3, the RV changes are largely of the same sign and of the same order of magnitude or sometimes slightly less pronounced, which is in contradiction to Hennessy et al. (1997) who report that under global warming conditions changes in extreme rainfall are usually stronger than changes in total accumulation because of the higher moisture holding capacity of warmer air masses. However, here we find that daily rainfall variability is largely stabilizing around a higher or lower mean.

Simulated heat waves are clearly intensifying in Subsaharan West Africa, except in boreal winter over the western SHZ (Fig. 11b). It appears obvious that the reduction in rainfall and cloud cover on the one hand and greater sensible heat fluxes associated with decreasing soil moisture on the other hand trigger extremely hot near-surface conditions, especially in JJA and SON. The highest amplitude is in a zone around 12°N, where precipitation totals are clearly diminishing (Figs. 3, 5). The weakening temperature extremes in winter over the western part of the Sahel may be related to an increase in surface albedo (Fig. 2), which offsets the effect of reduced evaporation during the dry season and in the absence of the solar maximum. The RV changes are more extreme than the mean changes as indicated by Fig. 6: for instance in the southern SHZ the mean summer climate is heating by less than 3°C, while the hottest day of the year 2025 is up to 6°C warmer than in 2000. McGuffie et al. (1999) have explained this behaviour through the impact of reduced soil moisture, leading to exorbitantly rising maximum temperatures in regions like tropical Africa.

5 Conclusions

The present study aims to provide a simulation of African climate change up to 2025 under fairly realistic assumptions concerning future land degradation and increasing GHG concentrations. Time slices simulated by means of a regional climate model at high spatio-temporal resolution are used to identify significant trends in the hydrological cycle, temperature, atmospheric circulation and climate extremes. The major part of tropical Africa may undergo much dryer climate conditions by 2025, with the largest anomalies occurring during the summer monsoon season (reductions of 100–500 mm), with reductions in vegetation cover and soil moisture providing the most relevant explanation. Accompanying a shift in the Bowen ratio towards less latent and more sensible heat fluxes from the land surface, lower-tropospheric temperature may increase considerably by up to 7°C. The surface heating may induce an intensification of the JJA monsoonal flow into tropical Africa, which is associated primarily with more moisture advection into the region. This leads to slightly enhanced large-scale precipitation but heavily reduced convective rainfall due to the substantial decrease in evapotranspiration. Simulated changes in daily extreme values over the period 2000–2025 usually take place in the same direction as the mean changes with less severe rainfall extremes in JJA but more intense heat waves in tropical Africa. In the case of temperature, the magnitude of climate extremes are affected more strongly than the mean climate. In the subtropical parts of Africa, the climate change signals are much weaker. During the winter rainy season in Morocco and over the Iberian Peninsula, rainfall amounts are also decreasing, albeit of lower amplitude, and positive temperature trends occur particularly in the High

Atlas region, which may result in less snow accumulation, which acts as an important storage component for the irrigation-based agriculture in Morocco.

There are several main conclusions to be drawn from this analysis: (1) The regional climate model simulations suggest a dryer and warmer climate in most of tropical Africa. Extreme events such as heat waves probably intensify and contribute to an overall deterioration of living conditions in Subsaharan Africa, except in some parts of the GCR where oceanic heating in the tropical Atlantic may lead to enhanced moisture convergence in summer and sufficient freshwater availability (Clark et al. 2001; Vizy and Cook 2001; Paeth and Stuck 2004). (2) There is evidence that land degradation may play a more important role in African climate change up to 2025 than GHG-induced radiative heating. (3) The response patterns of the hydrological cycle and temperature largely reflect the spatial distribution of high vegetation density during the seasonal cycle. This indicates that local changes in land cover are directly associated with local climate change. It is well known that the small-scale recycling of water – transferring local evapotranspiration directly to local moist convection and precipitation – represents an important component of the hydrological cycle in low latitudes. The fact that land degradation is a key factor influencing African climate change and that its local effect dominates the large-scale dynamical effects is potentially of high political relevance. It implies that protection and conservation measures at the local to national scale, including reforestation and land use controls, may result in more abundant freshwater input from rainfall, or at least in a mitigation of the negative implications of future climate. In the context of the interdisciplinary IMPETUS project, these results are intended to contribute to a decision support system, which is dedicated to improving the management of freshwater resources in Benin and Morocco. From a scientific point of view, it is clearly desirable and interesting to simulate African climate far beyond the year 2025. However, this would extend the analysis far beyond the usual scope for policy making, which is a chief concern in IMPETUS.

The experimental design used in this study still comprises some sources of uncertainty which need to be improved in further investigations. Specifically: (1) It has been shown that the preselected time slices are not universally representative of the transient climate changes imposed by land degradation and greenhouse forcing. Shorter-term climate variations, arising mainly from interannual variability in the global ECHAM4 input data, obscure the long-term trends at many grid points and hamper the detection of fingerprints in African climate change. One solution is to integrate the REMO experiments over many years into the future in order to enhance the degrees of freedom and to better isolate the transient climate trends from the background of internal variability. (2) The atmospheric input data is derived from only one realization of the ECHAM4 global climate model. A more reliable approach would involve the use of several ensemble members from ECHAM4, and possibly ensemble simulations from other climate models to force REMO and to interpret the mean changes in REMO with respect to all (multi-model) ensemble members, the range between the simulations serving as a measure of uncertainty (cf. Paeth and Hense 2002). (3) There is a potential for inconsistency between the land degradation simulated within the REMO domain and the global atmospheric forcing data, which are not aware of any changes in vegetation cover. All three uncertainty factors will be addressed in the near future thzrough the use of ensemble simulations with REMO extended over several decades into the twenty-first century and driven

by global climate model runs which include a fully interactive vegetation at the global scale.

Acknowledgements This work was supported by the Federal German Minister of Education and Research (BMBF) under grant No. 07 GWK 02 and by the Ministry of Science and Research (MWF) of the Federal State of Northrhine-Westfalia under grant No. 223-21200200. We thank four anonymous reviewers for their helpful comments and Charles Rogers for proofreading the English.

References

Bell JL, Sloan LC, Snyder MA (2004) Regional changes in extreme climatic events: a future climate scenario. J Climate 17:81–87

Benson C, Clay EJ (1998) The impact of drought on sub-Saharan economies. World Bank Tech Paper, No. 401, Wold Bank, Washingtion DC

Black E, Slingo J, Sperber KR (2003) An observatonal study of the relationship between excessively strong short rains in coastal East Africa and Indian Ocean SST. Mon Weather Rev 131:74–94

Bounoua L, Collatz GJ, Los SO, Sellers PJ, Dazlich DA, Tucker CJ, Randall DA (2000) Sensitivity of climate to changes in NDVI. J Climate 13:2277–2292

Camberlin P, Janicot S, Poccard I (2001) Seasonality and atmospheric dynamics of the teleconnection between African rainfall and tropical sea-surface temperature: Atlantic vs. ENSO. Int J Climatol 21:973–1004

Changnon SD (2003) Measures of economic impacts of weather extremes. Bull Am Meteorol Soc 84:1231–1235

Christoph M, Speth P, Bollig M, Burkhardt J, Diekkrüger B, Menz G, Rössler M, Schug W (2004) Effizienter und tragähiger Umgang mit Süßwasser anhand zweier Beispiele in Nordwest-bzw. Westafrika. In: Lozán JL, Graßl K, Hupfer P, Menzel L, Schönwiese C-D (Hrsg.): Warnsignal Klima: Genug Wasser für alle? Wissenschaftliche Auswertungen. Hamburg, 282–286

CIESIN (1996) Gridded population density of the world. Consortium for International Earth Science Information Network, Michigan

Clark DB, Xue Y, Harding RJ, Valdes PJ (2001) Modeling the impact of land surface degradation on the climate of tropical North Africa. J Climate 14:1809–1822

Cook KH (1999) Generation of the African easterly jet and its role in determining West African precipitation. J Climate 12:1165–1184

Cullen HM, de Menocal PB (2000) North Atlantic influence on Tigris-Euphrates streamflow. Int J Climatol 20:853–863

Desanker PV, Justice CO (2001) Africa and global climate change: critical issues and suggestions for further research and integrated assessment modeling. Clim Res 17:93–103

Douville H, Chauvin F, Broqua H (2001) Influence of soil moisture on the Asian and African monsoons. Part I: mean monsoon and daily precipitation. J Climate 14:2381–2402

Douville H, Planton S, Royer J-F, Stephenson DB, Tyteca S, Kergoat L, Lafont S, Betts SA (2000) Importance of vegetation feedbacks in doubled-CO_2 climate experiments. J Geophys Res 105:14841–14861

Eklundh L, Olsson L (2003) Vegetation index trends for the African Sahel 1982–1999. Geophys Res Lett 30, doi:10.1029/2002GL016772

Feddema JJ, Freire S (2001) Soil degradation, global warming and climate impacts. Clim Res 17: 209–216

Findley SE (1994) Does drought increase migration? A study of migration from rural Mali during the 1983–1985 drought. Int Migr Rev 28:539–553

Fontaine B, Philippon N, Trzaska S, Roucou R (2002) Spring to summer changes in the West African monsoon through NCEP/NCAR reanalyses (1968–1998). J Geophys Res 107, doi:10.1029/2001JD000834

Fowler HJ, Kilsby CG (2003) Implications of changes in seasonal and annual extreme rainfall. Geophys Res Lett 30, doi:10.1029/2003GL017327

Gaertner MA, Christensen OB, Prego JA (2001) The impact of deforestation on the hydrological cycle in the western Mediterranean: an ensemble study with two regional climate models. Clim Dyn 17:857–873

Gallée H, Moufouma-Okia W, Bechtold P, Brasseur O, Dupays I, Marbaix P, Messager C, Ramel R, Lebel T (2004) A high-resolution simulazion of a West African rainy season using a regional climate mode. J Geophys Res 109, doi:10.1029/2003JD004020
Gasse F (2001) Hydrological changes in Africa. Science 292:2259–2260
Gibson R, Kallberg P, Uppala S, Hernandez A, Nomura A, Serrano E (1997) ERA description. Re-Analysis Project Report Series No. 1, European Centre for Medium-Range Weather Forecasts (ECMWF). Reading, UK
Hagemann S, Botzet M, Dümenil L, Machenhauer B (1999) Derivation of global GCM boundary conditions from 1 km land use satellite data. Max-Planck-Inst f Meteor, Report No. 289, Hamburg
Hastenrath S (2000) Interannual and longer term variability of upper-air circulation over the tropical Atlantic and West Africa in boreal summer. Int J Climatol 20:1415–1430
Hennessy KJ, Gregory JM, Mitchell JFB (1997) Changes in daily precipitation under enhanced greenhouse conditions. Clim Dyn 13:667–680
Hosking JRM (1990) L-moments: analysis and estimation of distributions using linear combinations of order statistics. J R Stat Soc B 52:105–124
Houghton JT, Ding Y, Griggs DJ, Noguer M, Van der Linden PJ, Dai X, Maskell K, Johnson CA (eds) (2001) Climate Change 2001. The Scientific Basis. Cambridge
Hulme M, Doherty R, Ngara T, New M, Lister D (2001) African climate change: 1900–2100. Clim Res 17:145–168
Jacob D (2001) A note to the simulation of the annual and interannual variability of the water budget over the Baltic Sea drainage basin. Meteorol Atmos Phys 77:61–74
Jacob D, Van den Hurk BJJM, Andrae U, Elgered G, Fortelius C, Graham LP, Jackson SD, Karstens U, Koepken C, Lindau R, Podzun R, Rockel B, Rubel F, Sass BH, Smith R, Yang X (2001) A comprehensive model intercomparison study investigating the water budget during the PIDCAP period. Meteorol Atmos Phys 77:19–44
Janicot S, Trzaska S, Poccard I (2001) Summer Sahel-ENSO teleconnection and decadal time scale SST variations. Clim Dyn 18:303–320
Jenkins GS, Kamga A, Garba A, Diedhiou A, Morris V, Joseph E (2002) Investigating the West African climate system using global/regional climate models. Bull Am Meteorol Soc 83:583–595
Kharim VV, Zwiers FW (2000) Changes in extremes in an ensemble of transient climate simulations with a coupled atmosphere-ocean GCM. J Climate 13:3760–3788
Knippertz P, Christoph M, Speth P (2003) Long-term precipitation variability in Morocco and the link to the large-scale circulation in recent and future climate. Meteorol Atmos Phys 83:67–88
Krichak SO, Kishcha P, Alpert P (2002) Decadal trends of main Eurasian oscillations and the Eastern Mediterranean precipitation. Theor Appl Climatol 72:209–220
Latif M, Dommenget D, Dima M, Grötzner A (1999) The role of Indian Ocean sea surface temperature in forcing East African rainfall anomalies during December–January 1997/1998. J Climate 12:3497–3504
Le Barbé L, Lebel T, Tapsoba D (2002) Rainfall variability in West Africa during the years 1950–90. J Climate 15:187–202
Long M, Entekhabi D, Nicholson SE (2000) Interannual variability in rainfall, water vapor flux, and vertical motion over West Africa. J Climate 13:3827–3841
Los SO, Collatz GJ, Bounoua L, Sellers PJ, Tucker CJ (2001) Global interannual variations in sea surface temperature and land surface vegetation, air temperature, and precipitation. J Climate 14:1535–1576
Lotsch A, Friedl MA, Anderson BT (2003) Coupled vegetation-precipitation variability observed from satellite and climate records. Geophys Res Lett 30, doi:10.1029/2003GL017506
Maynard K, Royer J-F (2004a) Effects of "realistic" land-cover change on a greenhouse-warmed African climate. Clim Dyn 22:343–358
Maynard K, Royer J-F (2004b) Sensitivity of a general circulation model to land surface parameters in African tropical deforestation experiments. Clim Dyn 22:555–572
McGuffie K, Henderson-Sellers A, Holbrook N, Kothavala Z, Balachova O, Hoekstra J (1999) Assessing simulations of daily temperature and precipitation variability with global climate models for present and enhanced greenhouse climates. Int J Climatol 19:1–26
Meehl GA, Zwiers FW, Evans J, Knutson T, Mearns L, Whetton P (2000) Trends in extreme weather and climate events: issues related to modeling extremes in projections of future climate change. Bull Am Meteorol Soc 81:427–436
Mo K, Bell GD, Thiaw WM (2001) Impact of sea surface temperature anomalies on the Atlantic tropical storm activity and West African rainfall. J Atmos Sci 58:3477–3496

Nakicenovic N, 27 co-authors (2000) Special report on emission scenarios. Intergovernmental Panel on Climate Change, Cambridge
Nicholson SE (2001) Climatic and enviromental change in Africa during the last two centuries. Clim Res 17:123–144
Nicholson SE, Palao IM (1993) A re-evaluation of rainfall variability in the Sahel. Part I. Characteristics of rainfall fluctuations. Int J Climatol 13:371–389
Nicholson SE, Some B, Kone B (2000) An analysis of recent rainfall conditions in West Africa, including the rainy season of the 1997 El Niño and the 1998 La Niña years. J Climatol 13:2628–2640
Paeth H (2004) Key factors in African climate change evaluated by a regional climate model. Erdkunde 58:290–315
Paeth H, Born K, Jacob D, Podzun R (2005) Regional dynamic downscaling over West Africa: model evaluation and comparison of wet and dry years. Meteorol Z 14:349–367
Paeth H, Friederichs P (2004) Seasonality and time scales in the relationship between global SST and African rainfall. Clim Dyn 23:815–837
Paeth H, Hense A (2002) Sensitivity of climate change signals deduced from multi-model Monte Carlo experiments. Clim Res 22:189–204
Paeth H, Hense A (2004) SST versus climate change signals in West African rainfall: 20th century variations and future projections. Clim Change 65:179–208
Paeth H, Hense A (2006) On the linear response of tropical African climate to SST changes deduced from regional climate model simulations. Theor Appl Climatol 83:1–19
Paeth H, Stuck J (2004) The West African dipole in rainfall and its forcing mechanisms in global and regional climate models. Mausam 55:561–582
Pahari K, Murai S (1997) Simulation of forest cover map for 2025 and beyond using remote sensing and GIS. Proceedings of the GIS Development
Palmer TN, Räisänen J (2002) Quantifying the risk of extreme seasonal precipitation events in a changing climate. Nature 415:512–514
Park J-S, Jung H-S, Kim R-S, Oh J-H (2001) Modelling summer extreme rainfall over the Korean peninsula using Wakeby distribution. Int J Climatol 21:1371–1384
Rauthe M, Hense A, Paeth H (2004) A model intercomparison study of climate change signals in extratropical circulation. Int J Climatol 24:643–662
Rodriguez-Fonseca B, de Castro M (2002) On the connection between winter anomalous precipitation in the Iberian Peninsula and North West Africa and the summer subtropical Atlantic sea surface temperature. Geophys Res Lett 29, doi:10.1029/2001GL014421
Roeckner E, Arpe K, Bengtsson L, Christoph M, Claussen M, Dümenil L, Esch M, Giorgetta M, Schlese U, Schulzweida U (1996) The atmospheric general circulation model ECHAM-4: model description and simulation of present-day climate. Max-Planck-Inst f Meteorol, Report No. 218, Hamburg
Rowell DP (2003) The impact of Mediterranean SSTs on the sahelian rainfall season. J Climate 16:849–862
Ruiz-Barradas A, Carton JA, Nigam S (2000) Structure of interannual-to-decadal climate variability in the tropical Atlantic sector. J Climate 13:3285–3297
Saha K, Saha S (2001) African monsoons. Part I: climatological structure and circulation. Mausam 52:479–510
Saravanan R, Chang P (2000) Interaction between tropical Atlantic variability and El Niño-Southern Oscillation. J Climate 13:2177–2194
Schnitzler K-G, Knorr W, Latif M, Bader J, Zeng N (2001) Vegetation feedback on Sahelian rainfall variability in a coupled climate land-vegetation model. Max-Planck-Inst F Meteorol, Report No. 329, 13 pp
Semazzi FHM, Song Y (2001) A GCM study of climate change induced by deforestation in Africa. Clim Res 17:169–182
Sutton RT, Jewson SP, Rowell DP (2000) The elements of climate variability in the tropical Atlantic region. J Climate 13:3261–3284
Taylor CM, Lambin EF, Stephenne N, Harding RJ, Essery RLH (2002) The influence of land use change on climate in the Sahel. J Climate 15:3615–3629
Tiedtke M (1989) A comprehensive mass flux scheme for cumulus parameterization in large scale models. Mon Weather Rev 117:1779–1800
Trenberth KE, Dai A, Rasmussen RM, Parsons DB (2003) The changing character of precipitation. Bull Am Meteorol Soc 84:1205–1217

Ulbrich U, Christoph M (1999) A shift of the NAO and increasing storm track activity over Europe due to anthropogenic greenhouse gas forcing. Clim Dyn 15:551–559
UNEP (2003) Global environmental outlook 3. http://www.grida.no/geo/geo3/english/
Vizy EK, Cook KH (2001) Mechanisms by whioch Gulf of Guinea and Eastern North Atlantic sea surface temperature anomalies can influence African rainfall. J Climate 14:795–821
van den Hurk BJJM, Viterbo P, Los SO (2003) Impact of leaf area index seasonality on the annual land surface evaporation in a global circulation model. J Geophys Res 108, doi:10.1029/2002JD002846
von Storch H, Zwiers FW (1999) Statistical analysis in climate research. Cambridge University Press, Cambridge, UK
Voss R, May W, Roeckner E (2002) Enhanced resolution modelling study on anthropogenic climate change: changes in extremes of the hydrological cycle. Int J Climatol 22:755–777
Wang G, Eltahir AB (2000) Ecosystem dynamics and the Sahel drought. Geophys Res Lett 27: 795–798
Xue Y, Juang H-M, Li W-P, Prince S, DeFries R, Jiao Y, Vasic R (2004) Role of land surface processes in monsoon development: East Asia and West Africa. J Geophys Res 109, doi:10.1029/2003JD003556
Zeng N, Hales K, Neelin JD (2002) Nonlinear dynamics in a coupled vegetation-atmosphere system and implications for desert–forest gradient. J Climate 15:3474–3487
Zeng N, Neelin JD (2000) The role of vegetation-climate interaction and interannual variability in shaping the African Savanna. J Climate 13:2665–2670
Zeng N, Neelin JD, Lau K-M, Tucker CJ (1999) Enhancement of interdecadal climate variability in the Sahel by vegetation interaction. Science 286:1537–1540
Zhao M, Pitman AJ (2002) The impact of land cover change and increasing carbon dioxide on the extreme and frequency of maximum temperature and convective precipitation. Geophys Res Lett 29, doi:10.1029/2002GL013476
Zolina O, Kapala A, Simmer C, Gulev S (2004) Analysis of extreme precipitation over Europe from different reanalyses: a comparative assessment. Glob Planet Change 44:129–161